Ecological Indicators 74 (2017) 384–391

Contents lists available at ScienceDirect

Ecological Indicators

journal homepage: www.elsevier.com/locate/ecolind

Monitoring soil salinity via remote sensing technology under data scarce conditions: A case study from Turkey

Taha Gorji[a,*], Elif Sertel[b], Aysegul Tanik[a]

[a] Department of Environmental Engineering, Istanbul Technical University (ITU), Faculty of Civil Engineering, 34462, Maslak, Istanbul, Turkey
[b] Department of Geomatics Engineering, Istanbul Technical University (ITU), Faculty of Civil Engineering, 34462, Maslak, Istanbul, Turkey

ARTICLE INFO

Article history:
Received 20 September 2016
Received in revised form
20 November 2016
Accepted 28 November 2016
Available online 9 December 2016

Keywords:
Agriculture
Remote sensing
Salinity indices
Soil salinity
Tuz lake
Turkey

ABSTRACT

Due to its negative impacts on land productivity and plant growth, soil salinization is a significant problem particularly in arid and semi-arid regions of the world. Among the natural factors of soil salinization, parent materials including high amount of salts and minerals in soil structure, known as primary salinization, can be addressed. Conventional irrigation techniques and poor drainage systems are predominant human-induced activities that result in secondary salinization. Countries with especially dryland environment, face difficulty in providing adequate food for their rapidly increasing population since each year lots of cultivated land are abandoned due to adverse effects of primary and secondary soil salinization. Therefore, monitoring, mapping and predicting soil salinization is of utmost importance regarding lessening and/or preventing further increase in soil salinity through some protective measures. The subject of concern becomes even more pronounced particularly in agricultural lands as is the case in the vicinity of Tuz (Salt) Lake Region in Turkey. This research focuses mainly on multi-temporal monitoring of Tuz Lake Region in order to track changes in areas of salty spots in years 1990, 2002, 2006, 2011 and 2015. A total number of 25 Landsat-5 TM and Landsat-8 images obtained between 1990 and 2015 were analysed in this study. Field electrical conductivity (EC) measurements for 322 soil samples in year 2002 were checked; and 28 of these samples were selected for generating salinity maps representing areas in the vicinity of the lake. All satellite images were radiometrically and atmospherically corrected prior to classification. Following the pre-processing step, five soil salinity indices were applied on all satellite images. 28 soil samples were then overlaid on images in order to extract the exact index values related to soil samples and regression approach was used to relate satellite image-derived salinity indices and field measurements. Linear and exponential regression analyses were conducted separately as the next step for all indices based on data gathered in 2002. Salinity index (SI) $1 = \sqrt{B1 * B3}$ showed the best result with R^2 value of 0.93 and 0.83 for exponential and linear regression analysis, respectively. Salinity maps for years 1990, 2006, 2011 and 2015 were further produced utilizing the exponential and linear regression expressions attained for year 2002. Besides, this study detected land cover changes in the area from year 2000–2006, and from 2006 to 2012 by using CORINE land cover data to analyse the possible relationships between land cover change and salinity changes.

1. Introduction

Soil salinity negatively affects seed germination, crop productivity, soil and water quality specifically in semi-arid and arid regions of the world, resulting in loss of arable lands and soil degradation. It is ever-increasing at an alarming rate and is accepted as a widespread environmental problem endangering agricultural practices as thoroughly mentioned by scientists from various parts of the world at different time intervals (Zhu, 2001; Metternicht and Zinck, 2003; Zheng et al., 2009; Rongjiang and Jingsong, 2010). Generally, there are two main reasons for soil salinity. One relates to human-induced activities, and the other one is due to natural factors. Extent usage of poor quality irrigation water due to occurrence of extreme drought events combined with intense application of fertilizers are the main human-induced activities resulting in soil salinization (Perez-Sirvent et al., 2003; Barbouchi et al., 2014). Presence of parent materials and weathering of salt minerals by wind or water force are among the primary causes of soil salinization which is a common problem, and it becomes even more pronounced under high evaporation and less precipitation conditions (Metternicht and Zinck, 2008a). Mineral composition of

* Corresponding author.
E-mail addresses: tahagorji1@yahoo.com (T. Gorji), sertele@itu.edu.tr (E. Sertel), tanika@itu.edu.tr (A. Tanik).

http://dx.doi.org/10.1016/j.ecolind.2016.11.043
1470-160X/

soil, texture and its surface roughness are the core soil properties; whereby, physical properties of salinity varies by vegetation cover which is categorized as halophyte and non-halophyte plants (Metternicht and Zinck, 2003; Farifteh and Farshad, 2006). In fact, salt-affected regions could be differentiated from non-affected areas by the availability of halophytic plants indicating their characteristics of withstanding high soil salinity (Dehaan and Taylor, 2002; Fernández-Buces et al., 2006). Generally, photosynthetic activity of plants impact their spectral reflectance curve such a way that under less photosynthetic activity, plants have higher reflectance in visible and lower reflectance in near-infrared (NIR) portions of the spectrum from the vegetation, which is a case for crops facing salinity stress (Zhang et al., 2011).

Soil salinization is a process occurring dynamically with significant social and economic aspects; thus, for sustainable management of arable regions and natural ecosystems, proper and accurate information on spatial magnitude and variability in distribution of salinity is critical in order to timely monitor it and prevent further increase in salt-affected areas (Allbed and Kumar, 2013). Periodical monitoring of soil salinity is a necessity to properly manage soil and water resources; however, it is rather challenging to detect the required ground information in the regions impacted by salinity as referred by Gates et al. (2002) and Bilgili et al. (2011). United Nations Food and Agriculture Organization (FAO) have estimated that almost 397 million hectares of world's total land is covered by saline soil including nearly all continents (Koohafkan and Stewart, 2008).

Soil salinity has high spatio-temporal variability; therefore, it is important to monitor and map its changes to predict some natural disasters such as desertification and mitigate drastic environmental, social and economic consequences specifically for semi-arid and arid regions of the world. Extreme field study and sampling is needed to monitor and anticipate soil salinity by using conventional methods. Monitoring soil salinity by knowing when, where, and how salinity and sodicity may occur is significant for optimizing land productivity as underlined by Al-Khaier (2003). Remote Sensing (RS) techniques have been widely used to assess soil salinity since 1960s; while black-and-white, and coloured aerial photographs were utilized to map salt-affected soils. RS technology makes it possible to obtain multi-temporal data for varying spatial domains and conditions which is a key element to monitor and detect soil salinity (Gorji et al., 2015; Fan et al., 2015; Scudiero et al., 2015). There are some constrains in monitoring soil salinization due to dynamic processes occurring at the saline soil surface; whereby spectral, spatial and temporal behaviour of the salt features are affected (Metternicht and Zinck, 2008a). Therefore, spatial resolution of the satellite imagery is an essential parameter that should be considered while monitoring and tracking soil salinity (Metternicht and Zinck, 2008b). Proper detection and quantification of soil salinity can be achieved by utilizing digital indices derived from different spectral bands of satellite images and relating them to ground-based electromagnetic measurements of soil electrical conductivity (EC) as referred by a couple of researchers (Dehaan and Taylor, 2002; Fernández-Buces et al., 2006; Farifteh et al., 2008). Rapid and non-destructive detection, wide regional coverage and possibility for relatively inexpensive long-term monitoring can be counted among the advantages of RS technology (Allbed and Kumar, 2013; Kumar et al., 2015). Even though rapid and accurate assessment of soil salinity via RS has been improved progressively in the last decades, expanding in the existence of soil salinization under different parameters and variables forced researchers to accelerate in modelling this phenomenon (Akramkhanov, 2005; Vasques et al., 2009).

The main objective of this study is utilizing Remote Sensing (RS) and Geographical Information Systems (GIS) techniques to generate soil salinity maps in Tuz (Salt) Lake Region, Turkey, in order to track and monitor the changes in salt-affected areas in years 1990, 2002, 2006, 2011 and 2015. Besides, this study utilizes CORINE data for identifying probable human-induced causes of soil salinization in the area by detecting land cover changes from year 2000–2006 and from 2006 to 2012. In fact, information about land-use/land cover changes (LULC) is required to monitor these changes at various time intervals in order to make proper decisions to mitigate negative effects of these alterations on environment (Das, 2009). Fig. 1 illustrates the soil salinity map of the world where Turkey may be observed as a country that is not considerably affected by soil salinity problem; therefore, limited studies on monitoring and mapping soil salinity exist. In that sense, this article may be regarded as one of the rare studies conducted in the country that represents a developing country with limited field data.

2. Materials and methods

2.1. Study area

The study area, Tuz Lake and its vicinity, is located in Central Anatolia between longitude 32°59′–33°39′ and latitudes 38°20′–39°10′. It is the second largest lake in the country with spe-

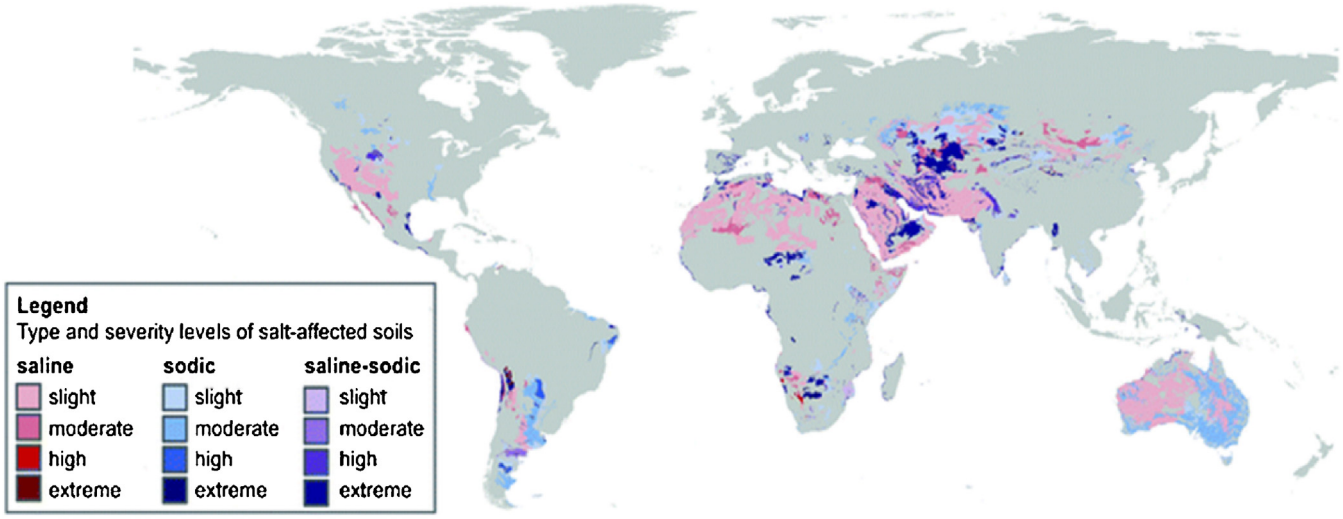

Fig. 1. Soil salinity map of the world (URL-1, 2016).

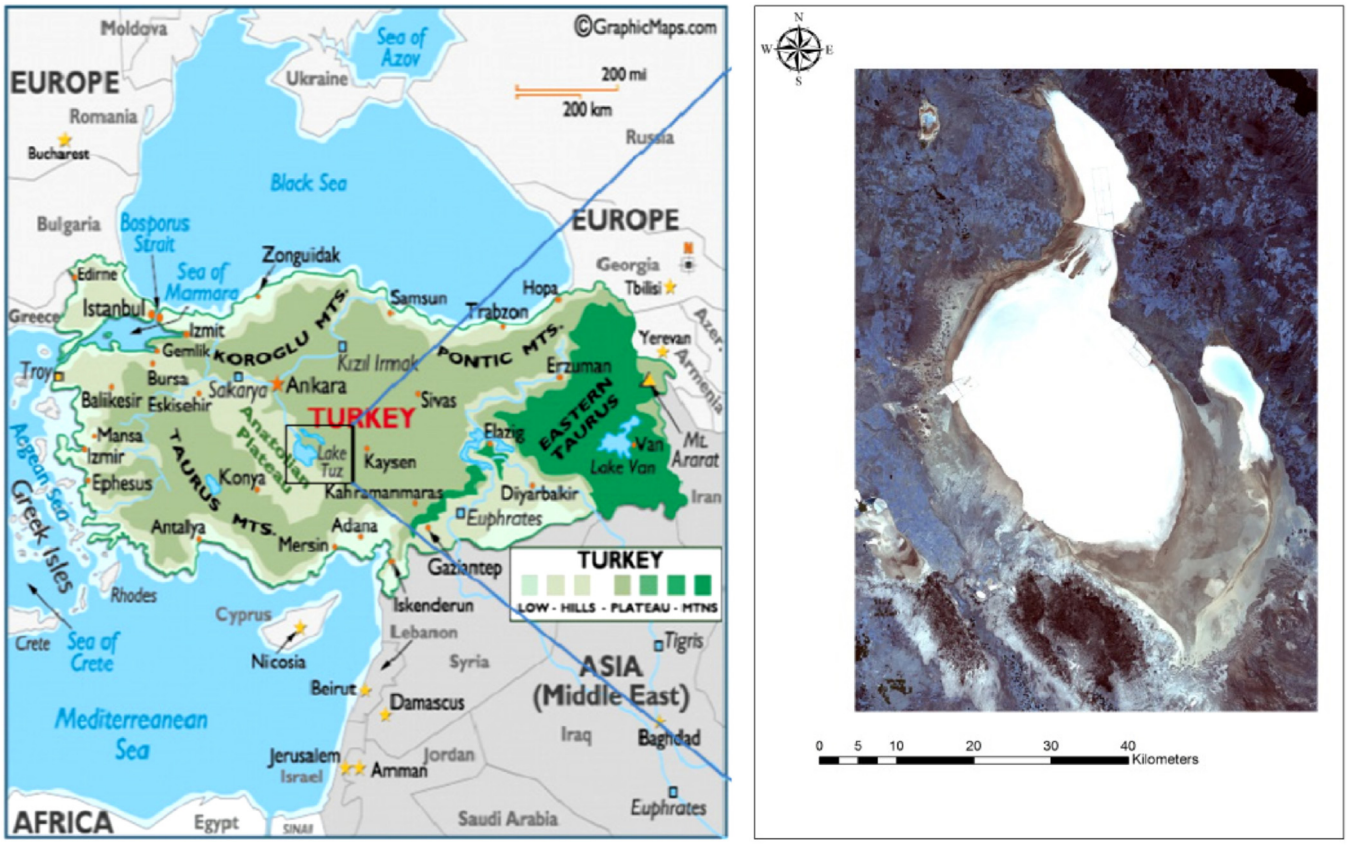

Fig. 2. Geographical location of Tuz Lake in Turkey.

cific kinds of flora and fauna. It occupies an area of about 1.500 km^2 with an altitude of 905 m (Ucan and Dursun, 2009). Tuz lake is mostly a shallow saline lake with an approximate length of 80 km land with a width of 50 km; but, during summer especially in July and August when the precipitation is less and temperature is high, it dries out exposing a salt flat (Kilic and Kilic, 2010). Agriculture, livestock breeding, salt production and tourism are the main human activities governing the economic conditions in the region (Mergen and Karacaoglu, 2015). The geographical location of the lake is illustrated coupled with a Landsat satellite image with a closer view in Fig. 2.

2.2. Data used for generating salinity maps

For generating soil salinity maps, monitoring multi-temporal changes in saline soils and detecting land-use/cover change in the study area, three groups of data were used; namely, four Landsat 5 images obtained in June 1990, 2002, 2006, 2011 and one Landsat 8 image obtained in June 2015 which were downloaded from United States Geological Survey (USGS) web site, Coordination of Information on the Environment (CORINE) land cover data of year 2000, 2006 and 2012 accessed from European Environmental Agency and, and field electrical conductivity (EC) measurements conducted by the Ministry of Agriculture of Turkish Republic. Totally, 28 field EC measurements were selected from a total number of 322 soil samples which were obtained during May–July 2002 in Tuz Lake basin. 28 of these sampling points, geographically representing the vicinity of the lake (area of interest used in this research) with various EC ranges, were selected to create relationship between field data and satellite image-derived salinity indices. Data scarcity is a typical characteristic problem in developing countries like in Turkey where sampling and field measurements were conducted just once in year 2002 within the framework of a national project conducted by the Republic of Turkey Ministry of Food, Agriculture and Livestock on the determination of alternative agricultural practices and quality classification of soil and land at Tuz Lake Special Protection Area. Regarding the CORINE data, two sets of vector data were selected for detecting land cover changes in the study area. One is related to changes from 2000 to 2006, and the other one is associated with alteration from 2006 to 2012.

2.3. Methodology used

Satellite images were radiometrically and atmospherically corrected to minimize radiometric distortions and atmospheric perturbations caused by clouds, aerosols and other atmospheric particles, respectively (Tempfli et al., 2009). Regarding the Landsat satellite images, the effect of water vapour absorption is significant for the TM/ETM+'s near- infrared (IR) channels (Liang et al., 2001), therefore, atmospheric correction is necessary to determine true surface reflectance values in order to retrieve them accurately. After pre-processing, salinity indices were utilized for categorizing salinity classes based on assigning corresponding pixel values to EC values, and finally regression analysis has been conducted for finding relationship between ground EC measurements and satellite images index values. Resultantly, soil salinity maps were generated. In order to produce the maps including five salinity classes (non-saline, slightly saline, moderately saline, highly saline and extremely saline) for Tuz Lake region, five soil salinity indices were applied to images belonging to years 1990, 2002, 2006, 2011 and 2015. Table 1 shows the set of salinity indices used for generating the salinity maps. Parameters B1, B2, B3 and B4 used in indices are abbreviated for Band1, Band2, Band3 and Band4 of Landsat

Table 1
Soil salinity indices used for generating salinity maps.

Salinity Index (SI)	Description	References
SI 1 = $\sqrt{B1 * B3}$	B1 = Band 1 - Blue, B3 = Band 3 - Red	(Khan et al., 2005)
SI 2 = $\sqrt{B2 * B3}$	B2 = Band 2- Green, B3 = Band 3 - Red	(Khan et al., 2005)
SI 3 = $\sqrt{(B2)^2 + (B3)^2 + (B4)^2}$	B2 = Band 2- Green, B3 = Band 3 - Red, B4 = Band 4 - Near Infrared	(Douaoui et al., 2006)
SI 4 = $\sqrt{(B2)^2 + (B3)^2}$	B2 = Band 2- Green, B3 = Band 3 - Red	(Douaoui et al., 2006)
SI 5 = $\sqrt{(B3)^2 + (B4)^2}$	B3 = Band 3 – Red, B4 = Band 4 - Near Infrared	(Khan et al., 2005)

Table 2
Soil salinity classes and their effect on crops (Brown et al., 1954).

Salinity class	EC (dS/m)	Salinity effects on crops
Non-saline	0–2	Salinity effects are negligible
Slightly saline	2–4	Yield loss for very sensitive crops
Moderately saline	4–8	Many crops are affected and their yield is restricted
Highly saline	8–16	Only tolerant crops bear this condition
Extremely saline	>16	Only a few very tolerant crops resist

satellite representing Blue, Green, Red and Near Infrared portion of electromagnetic spectrum, respectively.

After applying each index for the satellite images of different years, pixel values with various ranges in all images were extracted. Corresponding EC values were then compared with their exact pixel value of the same location. The output images, as a result of index calculation, were imported to GIS environment to create soil salinity map based on level slicing approach of different index ranges and to integrate these maps with CORINE Land Use and Land Cover (LULC) maps. Universal Transverse Mercator (UTM) with Zone 36 N was used as projection system and World Geodetic System (WGS-1984) was used as datum during the research to make all geographic data compliant with each other. Corresponding pixel values for each field sample locations were then extracted to create relationship. Classes were defined based on appointing proper pixel values to EC values of 2 dS/m, 4 dS/m, 8 dS/m and 16 dS/m to relate them with the degree of salinity. Table 2 shows the salinity classes and their corresponding effects on crops.

A particular relationship between ground data (EC values) measured in the field and salinity index values derived from satellite images is required for generating soil salinity maps and for assessing the categorization of salinity classes. Therefore, in this study, two different approaches; namely, linear regression analysis and exponential regression analysis have been conducted to establish a relationship between field data and satellite image-derived indices. EC value was used as dependent variable; whereas, index values derived from satellite images were used as independent variable. EC values were estimated for unmeasured locations by using the known salinity index values of the same location based on the generated plots. Relationship between EC values of 28 sampling sites and values of indices from satellite images were provided via a formula which can be used to find out EC values for the entire study area. Each pixel index value was inserted into the regression equation, and possible EC value for that pixel location was calculated. Both linear and exponential regression analyses have been conducted on the available satellite images through which maps were separately generated by different salinity indices of using the ground data belonging to year 2002. In fact, the model was established for year 2002, since both EC ground data and satellite images existed simultaneously at that specific year.

Table 3
CORINE land cover changes from 2000 to 2006.

CLC in 2000	CLC in 2006	Areal change (ha)
Sparsely vegetated areas	Permanently irrigated land	44
Natural grasslands	Permanently irrigated land	1595
Natural grasslands	Non-irrigated arable land	3746
Non-irrigated arable land	Industrial units	8
Natural grasslands	Industrial units	7
Total		5400

Table 4
CORINE land cover changes from 2006 to 2012.

CLC in 2006	CLC in 2012	Areal change (ha)
Non-irrigated arable land	Pastures	236
Non-irrigated arable land	Industrial units	18
Pastures	Construction sites	24
Permanently irrigated land	Pastures	22
Pastures	Non-irrigated arable land	104
Total		404

Table 5
Exponential regression analysis results for five different salinity indices.

Salinity Index (SI)	Index Range	Date of Satellite Image	Number of Samples	R^2
SI 1 = $\sqrt{B1 * B3}$	0–1	25.06.2002	28	0,93
SI 2 = $\sqrt{B2 * B3}$	0–1	25.06.2002	28	0,90
SI 3 = $\sqrt{(B2)^2 + (B3)^2 + (B4)^2}$	0–1.73	25.06.2002	28	0,87
SI 4= $\sqrt{(B2)^2 + (B3)^2}$	0–1.42	25.06.2002	28	0,89
SI 5= $\sqrt{(B3)^2 + (B4)^2}$	0–1.42	25.06.2002	28	0,82

2.4. Investigation of CORINE data

CORINE Land Cover (CLC) data is data of the European environmental landscape based on interpretation of satellite images. It is a necessary tool for providing proper and extensive information for both decision-makers and administrative managers engaged in resource management and sustainable development. Human-induced activities such as expanding agricultural lands for food supply, rapid population growth and urbanization, advances in technology and economic development are the significant factors affecting land cover changes. Besides, natural causes such as climate change and drought also have impact on land cover changes (URL-2, 2016).

For this study, CORINE CLC data for years 2000, 2006 and 2012 were analysed for the Tuz Lake Region in consideration of CLC change detection as shown in Fig. 3. Also, two working units from CORINE 2006 data for Turkey were used to determine land cover classes in the Lake Region. All classes with their corresponding areas were calculated after importing CORINE data to ArcGIS 10.2.1 software. Besides, land cover changes were analysed using CORINE change shape file for years 2000, 2006 and 2012. The main changes were related to conversion of natural grassland and vegetated areas to agricultural arable land from 2000 to 2006, and then conversion of agricultural arable land to pastures and artificial surfaces from 2006 to 2012 as given in Table 3 and Table 4, respectively. The most noticeable CLC occurred in the period of 2000–2006 with an area of 5400 ha compared to the second inspection period of 2006–2012 where the land alteration is limited to 404 ha.

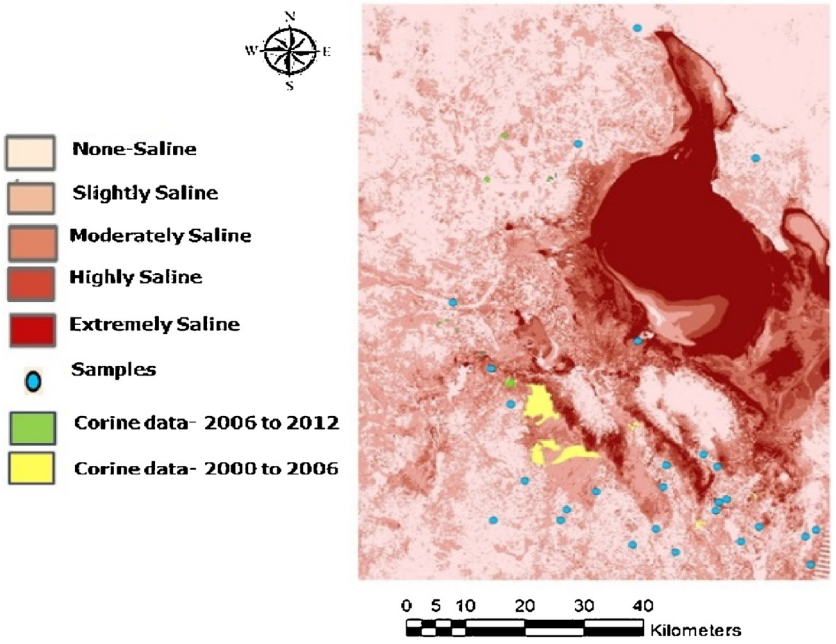

Fig. 3. CORINE CLC Map of Tuz Lake.

Table 6
Linear regression analysis results for five different salinity indices.

Salinity Index (SI)	Index Range	Date of Satellite Image	Number of Samples	R^2
SI 1 = $\sqrt{B1 * B3}$	0–1	25.06.2002	28	0,83
SI 2 = $\sqrt{B2 * B3}$	0–1	25.06.2002	28	0,77
SI 3 = $\sqrt{(B2)^2 + (B3)^2 + (B4)^2}$	0–1.73	25.06.2002	28	0,76
SI 4= $\sqrt{(B2)^2 + (B3)^2}$	0–1.42	25.06.2002	28	0,74
SI 5= $\sqrt{(B3)^2 + (B4)^2}$	0–1.42	25.06.2002	28	0,71

Table 7
Linear regression analysis results for several salinity indices used in Central Morocco (Lhissou et al., 2014).

Spectral indices	Equation	R^2	Results of this study R^2
Brightness Index (BI)	$\sqrt{(B3)^2 + (B4)^2}$	0.47	0.71
Salinity index (SI) 1	$\sqrt{B1 * B3}$	0.68	0.83
SI 2	$\sqrt{B2 * B3}$	0.55	0.77
SI 4	$\sqrt{(B2)^2 + (B3)^2}$	0.53	0.74
SI 5	B5/B7	0.06	–
SI 6	(B5-B7)	0.5	–

3. Results and discussion

Exponential and linear regression results for 5 different salinity indices of year 2002 were illustrated in Table 5 and Table 6, respectively. Salinity index (SI) 1 = $\sqrt{B1 * B3}$ indicated the best result with R^2 value 0.93 and 0.83 for the exponential and linear regression analysis in turn. Exponential regression equation $y = 0.1372e^{6.8658x}$ and linear regression equation y = 49.144 x – 15.909 were used to calculate the corresponding salinity index values, 'x' values, for EC measurements of 2, 4, 8 and 16 by inserting these values as 'y' in the equation. Calculated 'x' values were then used to predict EC salinity maps for different years as shown in Figs. 4 and 5.

Exponential regression analysis has been conducted in some other case studies depicted in literature. In the District Faisalabad, the Central Punjab of Pakistan, researchers utilized Indian Remote Sensing (IRS) satellite images for establishing empirical relationships or models using indices such as (SI) 1 = $\sqrt{B1 * B3}$ and ground truth data. An exponential function of 3rd order was found as highly promising with significant results (Abbas et al., 2013). Linear regression analysis has also been conducted in various case studies as a step towards generating soil salinity maps. In El-Tina Plain located on the North-western Sinai Peninsula in Egypt, researchers utilized two predictive models; namely, Partial Least Squares Regression (PLSR) and Multivariate Adaptive Regression Splines (MARS) based on the measured EC and laboratory soil reflectance spectra resampled to Landsat sensor's resolution. The result for PLSR and MARS linear regression analysis resulted in R^2 value of 0.73 and 0.70, respectively. These findings were quite satisfactory for predicting new EC value for different spots in various years (Nawar et al., 2014). Another study conducted in Central Iraq for mapping soil salinity put forth multi-temporal changes by applying Generalized Difference Vegetation Index (GDVI) to Landsat 4, Landsat 5 and Landsat 7 ETM+ images that resulted in R^2 value of 0.94 (Wu et al., 2014). In the Lower Cliff Plain of Algeria, researchers utilized five soil salinity indices namely SI 1 = $\sqrt{B1 * B3}$, SI 2 = 2*B2-(B3 + B4), SI 3= $\sqrt{(B2)^2 + (B3)^2}$, SI 4 = (B3-B4)/(B3+B4) and Soil Adjusted Salinity Index (SASI) = B3/(100*(B1)$\hat{2}$) on Landsat 7 images in order to detect and predict soil salinity in the region Yahiaoui et al. (2015). They also generated multiple linear regression model for soil salinity prediction based on elevation and the Soil Adjusted Salinity Index (SASI) = B3/(100*(B1)$\hat{2}$) with R^2 value of 0.45 between measured EC and predicted EC (Zhang et al., 2015). Furthermore, in Tadla-Azilal Region of Central Morocco, several soil salinity indices depicted in Table 7 were applied on Landsat TM satellite images to detect and map soil salinization. The best result similar to this research was obtained for (SI) 1 = $\sqrt{B1 * B3}$ with R^2 value equal to 0.68 (Lhissou et al., 2014).

In another study conducted in Yellow River Delta situated on the Northeast coast of China, soil salinity was detected by means of Moderate Resolution Imaging Spectroradiometer (MODIS) and by utilizing Enhanced Vegetation Index (EVI). The relationship between plant biomass and salt stress were investigated using linear regression method. Biomass decreased linearly with the

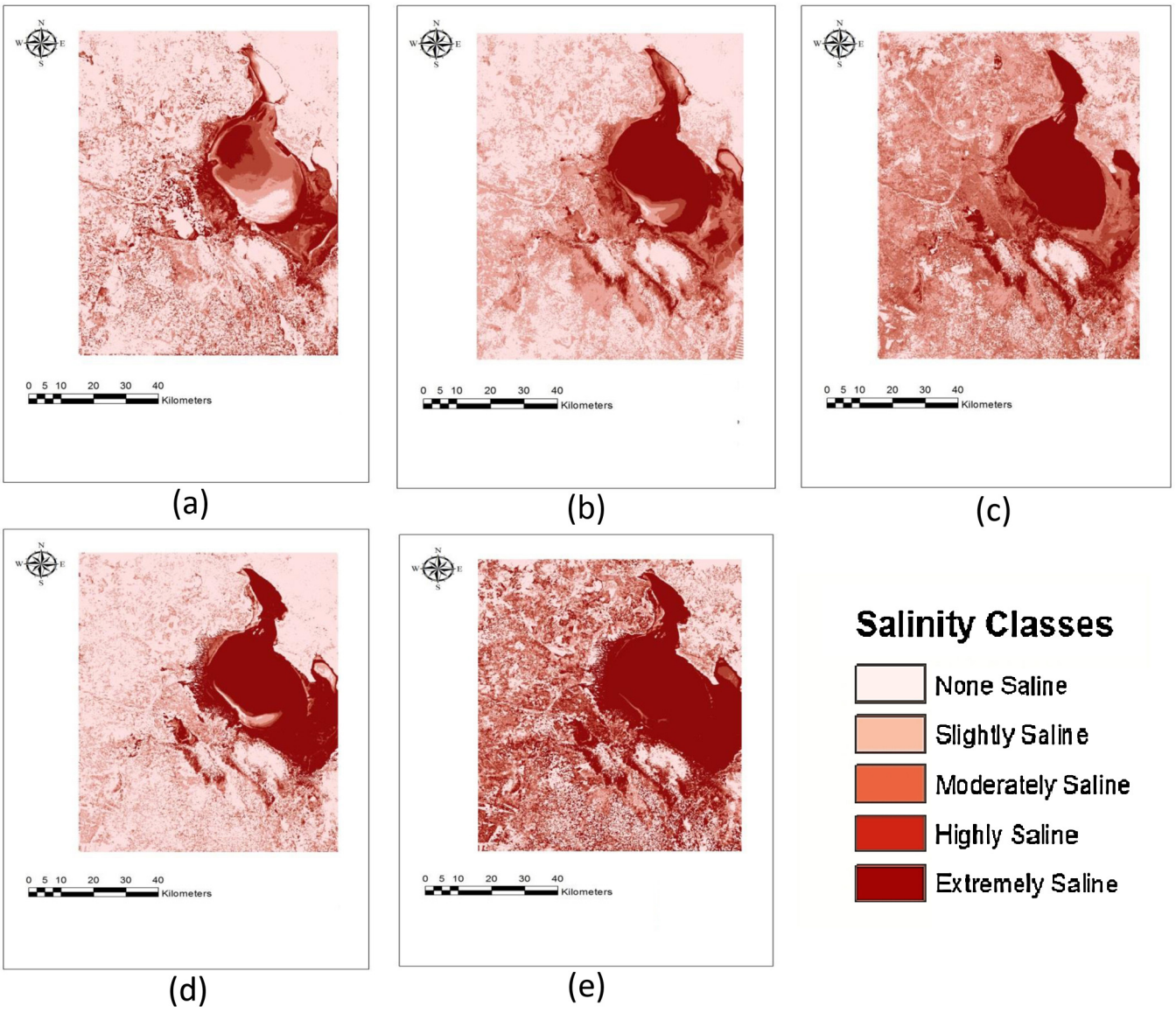

Fig. 4. Salinity maps of Tuz Lake Region as a result of salinity Index (SI) $1=\sqrt{B1 * B3}$ and exponential regression analysis: (a) 1990, (b) 2002, (c) 2006, (d) 2011, (e) 2015.

increased soil salinity in cropland, and the linear regression model resulted in R^2 value of 0.85 (Zhang et al., 2015). Regional scale soil salinity evaluation using Landsat 7 was conducted in California, USA where researchers found EC ground-truth relationship with Landsat 7 reflectance after applying SI = (B2*B3)Ô0.5 and the result showed R^2 value of 0.85 (Scudiero et al., 2014).

As such, review of similar case studies and the outputs of this study indicated that utilizing modern tools of technology like RS, GIS and regression analyses enable detecting, monitoring and mapping salinity changes and levels of salinity on large areas with ease and more importantly, at low cost and time. The regression analyses, either linear or exponential, outperform quite reliable results varying according to the location of the inspected areas. Therefore, it is recommended for the scientists to try an extended number of SI's for their specific areas, and then, select the one that results in comparatively higher R^2. The results obtained from this study indicated that both linear (0.71–0.83) and exponential (0.82–0.93) regression analyses put forth satisfactory R^2 statistics; however, the best model-fit belonged to S1 with 0.93 for exponential analysis. These outcomes also lie within the statistic ranges of the other similar studies conducted at different parts of the world.

4. Conclusions and recommendations

Soil salinization is not as controversial as the other environmental issues like global warming, climate change, water pollution and scarcity, air pollution and deforestation; but it should not be underestimated since it is understood that if soil salinization increases in future with its present rate, a lot of countries will suffer from producing enough food for their population. Most current studies have nowadays focused on differentiating salinized soil and non-salinized soil, qualitatively analysing the distribution of soil salinity and monitoring the dynamics of soil salinity.

In recent years, RS, GIS and modelling have become the preferred technological tools to map soil salinity due to large area coverage which is of utmost importance both from the agricultural and environmental perspectives. After reviewing various case studies related to soil salinization, a case study for generating salinity maps in Tuz Lake Region was conducted by utilizing five different salinity index and two types of regression analysis in order to detect multi-temporal soil salinity changes from year 1990–2015. In addition, results of land cover changes using CORINE data indicated minor land-use changes by human-induced activities from

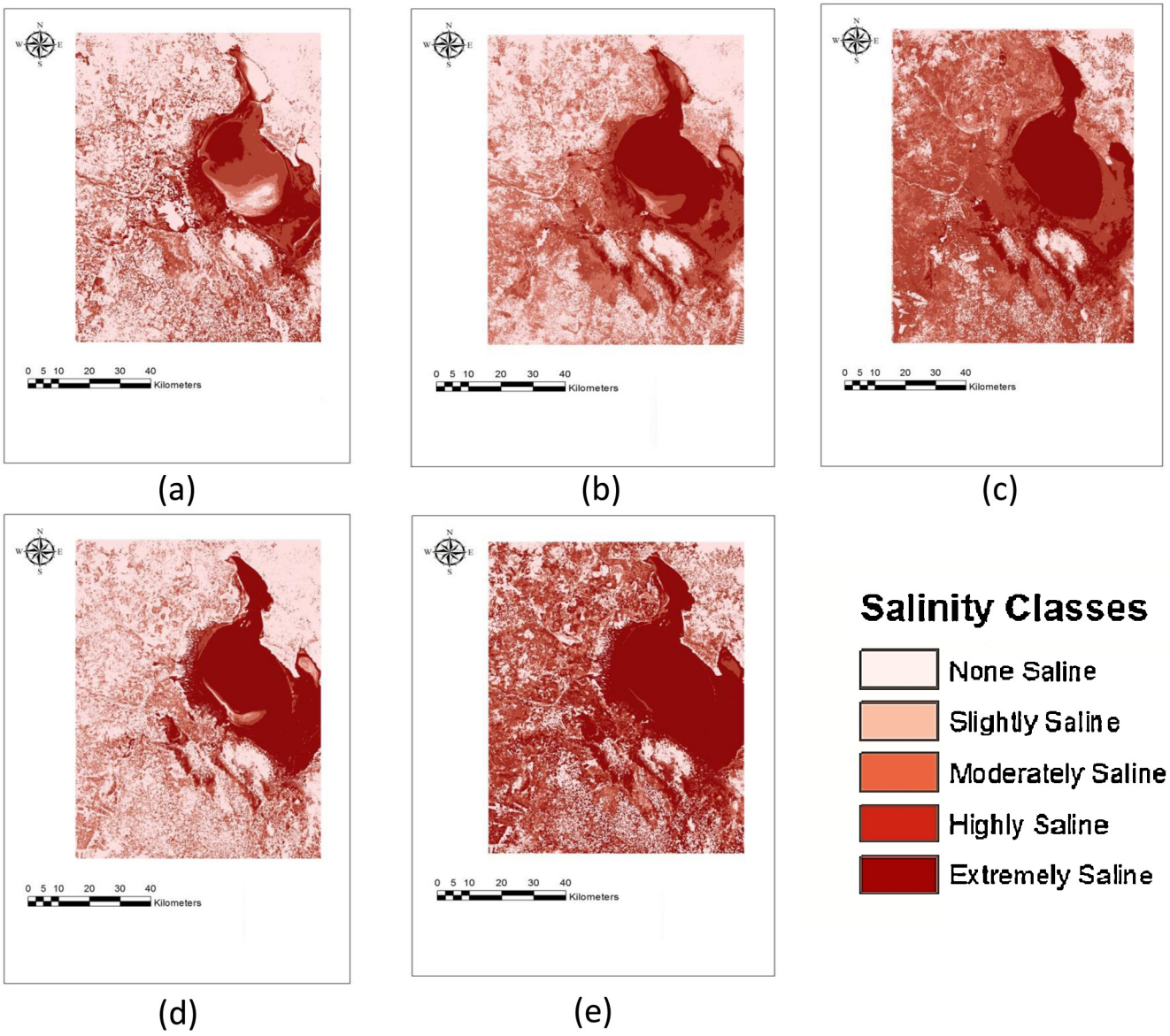

Fig. 5. Salinity maps of Tuz Lake Region as a result of salinity Index (SI) $1=\sqrt{B1 * B3}$ and linear regression analysis: (a) 1990, (b) 2002, (c) 2006, (d) 2011, (e) 2015.

year 2000–2012. Therefore, it can be concluded that soil salinization in the region was basically due to natural causes during this time period. Regarding the future studies, it is recommended to conduct further research on the tasks for cultivating halophilic plants in lands which are highly saline and as a result salt-tolerant plant can be effective for reclamation of saline soils in the area.

References

Abbas, A., Khan, S., Hussain, N., Hanjra, M.A., Akbar, S., 2013. Characterizing soil salinity in irrigated agriculture using a remote sensing approach. Phys. Chem. Earth. 55-57 (Parts A/B/C), 43–52.

Akramkhanov, A., 2005. The Spatial Distribution of Soil Salinity: Detection and Prediction. ZEF Ecology and Development. Cuvillier Verlag, Göttingen (Series No. 32, ISBN-3-86537-654-1).

Al-Khaier, F., 2003. Soil Salinity Detection Using Satellite Remote Sensing. Geo-Information Science and Earth Observation, http://www.itc.nl/library/papers_2003/msc/wrem/khaier.pdf (Accessed 20.06.2016).

Allbed, A., Kumar, L., 2013. Soil salinity mapping and monitoring in arid and semi-Arid regions using remote sensing technology: a review. Adv. Remote Sens. 2, 373–385.

Barbouchi, M., Abdelfattah, R., Member, S., Chokmani, K., Aissa, N. Ben, Lhissou, R., El Harti, A., 2014. Soil salinity characterization using polarimetric InSAR coherence: case studies in Tunisia and Morocco. IEEE J. Sel. Top. Appl. Earth Obs. Remote Sens., 1–10.

Bilgili, A.V., Cullu, M.A., Es, H., Van, Aydemir, A., Bilgili, A.V., Cullu, M.A., Van Es, H., 2011. The use of hyperspectral visible and near infrared reflectance spectroscopy for the characterization of salt-Affected soils in the harran plain, Turkey. Arid Land Res. Manag. 25 (1), 19–37.

Brown, J.W., Hayward, H.E., Richards, A., Bernstein, L., Hatcher, J.T., Reeve, R.C., Richards, L.A., 1954. Diagnosis and Improvement of Saline and Alkali Soils, 60. United States Department of Agriculture, Agriculture handbook.

Das, T., 2009. Land Use/Land Cover Change Detection: an Object Oriented, Thesis, Master of Science in Geospatial Technologies. Institute for Geoinformatics University of Münster.

Dehaan, R.L., Taylor, G.R., 2002. Field-derived spectra of salinized soils and vegetation as indicators of irrigation-induced soil salinization. Remote Sens. Environ. 80, 406–417.

Douaoui, A.E.K., Nicolas, H., Walter, C., 2006. Detecting salinity hazards within a semi-arid context by means of combining soil and remote-sensing data. Geoderma 134 (1–2), 217–230.

Fan, X., Liu, Y., Tao, J., Weng, Y., 2015. Soil salinity retrieval from advanced multi-Spectral sensor with partial least square regression. Remote Sens. 7 (1), 488–511.

Farifteh, J., Farshad, A., George, R.J., 2006. Assessing salt-affected soils using remote sensing, solute modelling, and geophysics. Geoderma 130 (3–4), 191–206.

Farifteh, J., Van Der Meer, F., Van Der Meijde, M., Atzberger, C., 2008. Spectral characteristics of salt-affected soils A laboratory experiment. Geoderma 145, 196–206.

Fernández-Buces, N., Siebe, C., Cram, S., Palacio, J.L., 2006. Mapping soil salinity using a combined spectral response index for bare soil and vegetation: a case study in the former lake Texcoco, Mexico. J. Arid Environ. 65 (4), 644–667.
Gates, T.K., Asce, M., Burkhalter, J.P., Asce, M., Labadie, J.W., Asce, M., Broner, I., 2002. Monitoring and modeling flow and salt transport in a salinity-threatened irrigated valley. J. Irrig. Drain. Eng. 128, 87–99.
Gorji, T., Tanik, A., Sertel, E., 2015. Soil salinity prediction, monitoring and mapping using modern technologies. Procedia Earth Planet. Sci. 15, 507–512.
Khan, N.M., Rastoskuev, V.V., Sato, Y., Shiozawa, S., 2005. Assessment of hydrosaline land degradation by using a simple approach of remote sensing indicators. Agric. Water Manage. 77 (1–3), 96–109.
Kilic, O., Kilic, A.M., 2010. Salt crust mineralogy and geochemical evolution of the Salt Lake (Tuz Gölü). Turkey Sci. Res. Essays 5 (11), 1317–1324.
Koohafkan, P., Stewart, B.A., 2008. Water and Cereals in Drylands. The Food and Agriculture Organization of the United Nations and Earthscan.
Kumar, S., Gautam, G., Saha, S.K., 2015. Hyperspectral remote sensing data derived spectral indices in characterizing salt-affected soils: a case study of Indo-Gangetic plains of India. Environ. Earth Sci. 73 (7), 3299–3308.
Lhissou, R., El Harti, A., Chokmani, K., 2014. Mapping soil salinity in irrigated land using optical remote sensing data. Eurasian J. Soil Sci. 3, 82–88.
Liang, S., Member, S., Fang, H., Chen, M., 2001. Atmospheric correction of landsat ETM + land surface imagery – part I: methods. IEEE Trans. Geosci. Remote Sens. 39 (11), 2490–2498.
Mergen, O., Karacaoglu, C., 2015. Tuz lake special environment protection area, central anatolia, Turkey: the EUNIS habitat classification andhabitat change detection between 1987 and 2007. Ekoloji 24 (95), 1–9.
Metternicht, G.I., Zinck, J.A., 2003. Remote sensing of soil salinity: potentials and constraints. Remote Sens. Environ. 85, 1–20.
Metternicht, G.I., Zinck, J.A., 2008a. Remote sensing of soil salinization: impact on land management. In: Shrestha, D.P., Farshad, A. (Eds.), Mapping Salinity Hazard: An Integrated Application of Remote Sensing and Modeling-Based Techniques. , 1st ed. Taylor & Francis Group, LLC, pp. 257–272.
Metternicht, G.I., Zinck, J.A., 2008b. Remote sensing of soil salinization: impact on land management. In: Schmid, T., Koch, M. (Eds.), Applications Ofhyperspectral Imagery to Soil Salinity Mapping. , 1st ed. Taylor & Francis Group, LLC, pp. 113–137.
Nawar, S., Buddenbaum, H., Hill, J., Kozak, J., 2014. Modeling and mapping of soil salinity with reflectance spectroscopy and landsat data using two quantitative methods (PLSR and MARS). Remote Sens. 6 (11), 10813–10834.
Perez-Sirvent, C., Martınez-Sanchez, M.J., Vidal, J., Sanchez, A., 2003. The role of low-quality irrigation water in the desertification of semi-arid zones in Murcia, SE Spain. Geoderma 113, 109–125.
Rongjiang, Y., Jingsong, Y., 2010. Quantitative evaluation of soil salinity and its spatial distribution using electromagnetic induction method. Agric. Water Manage. 97 (12), 1961–1970.
Scudiero, E., Skaggs, T.H., Corwin, D.L., 2014. Regional scale soil salinity evaluation using landsat 7, western san joaquin valley, california, USA. Geoderma Reg. 2-3, 82–90.
Scudiero, E., Skaggs, T.H., Corwin, D.L., 2015. Regional-scale soil salinity assessment using Landsat ETM+ canopy reflectance. Remote Sens. Environ. 169, 335–343.
Tempfli, K., Kerle, N., Huurneman, G.C., Janssen, L.L.F., Bakker, W.H., Feringa, W., Woldai, T., 2009. Principles of Remote Sensing, An Introductory Textbook, the International Institute for Geo-information Science and Earth Observation. University of Twente Faculty of Geo-Information and Earth Observation (ITC), pp. 56–85 (Chapter: 2. 2-2.4).
URL-1, 2016. https://globusgreen.wordpress.com/category/desertification/ (Accessed 07.08.2016).
URL-2, 2016. http://www.eea.europa.eu/publications/COR0-landcover/ (Accessed 06.09.2016).
Ucan, H.N., Dursun, S., 2009. Environmental problems of tuz lake (Konya-Turkey). J. Int. Environ. Appl. Sci. 4 (2), 231–233.
Vasques, G.M., Grunwald, S., Harris, W.G., 2009. Spectroscopic models of soil organic carbon in florida, USA. J. Environ. Qual. 39, 923–934.
Wu, W., Mhaimeed, A.S., Al-Shafie, W.M., Ziadat, F., Dhehibi, B., Nangia, V., De Pauw, E., 2014. Mapping soil salinity changes using remote sensing in Central Iraq. Geoderma Reg. 2-3, 21–31.
Yahiaoui, I., Douaoui, A., Zhang, Q., Ziane, A., 2015. Soil salinity prediction in the Lower Cheliff plain (Algeria) based on remote sensing and topographic feature analysis. J. Arid Land 7 (6), 794–805.
Zhang, T., Zeng, S., Gao, Y., Ouyang, Z., Li, B., Fang, C., Zhao, B., 2011. Using hyperspectral vegetation indices as a proxy to monitor soil salinity. Ecol. Indic. 11, 1552–1562.
Zhang, T.-T., Qi, J.-G., Gao, Y., Ouyang, Z.-T., Zeng, S.-L., Zhao, B., 2015. Detecting soil salinity with MODIS time series VI data. Ecol. Indic. 52, 480–489.
Zheng, Z., Zhang, F., Ma, F., Chai, X., Zhu, Z., 2009. Geoderma Spatiotemporal changes in soil salinity in a drip-irrigated field. Geoderma 149 (3–4), 243–248.
Zhu, J., 2001. Plant salt tolerance. Trends Plant Sci. 6 (2), 66–71.